Journal of Sol-Gel Science and Technology (2022) 101:571–578
https://doi.org/10.1007/s10971-022-05735-x

ORIGINAL PAPER: SOL-GEL AND HYBRID MATERIALS FOR BIOLOGICAL AND HEALTH (MEDICAL) APPLICATIONS

Preparation of PVA/starch hydrogel and its in-vitro drug release potential against pus-inducing pathogenic strain and breast cancer cell line

P. Sankarganesh[1] · V. Parthasarathy[2] · A. Ganesh Kumar[3] · S. Ragu[3] · M. Saraniya[3] · N. Udayakumari[3]

Received: 12 October 2021 / Accepted: 23 January 2022 / Published online: 9 March 2022

Abstract

The starch was blended with poly(vinyl) alcohol (PVA) to develop PVA/starch (PS) hydrogel. The physical interaction of PVA with starch was concluded by FTIR and XRD techniques. The thermal decomposition behavior of PS hydrogel was analyzed by thermogravimetric analysis. The swelling index and moisture loss analysis was carried out to comprehend the water absorption and retention behavior of PS hydrogel. The PS hydrogel was biocompatible with RBC due to its lower hemolysis value. The curcumin-loaded PS hydrogel showed an excellent anticancer activity against breast cancer cell line. The antibacterial activity of cephalosporin-loaded PS hydrogel was evaluated against the *Staphylococcus aureus*.

Graphical abstract

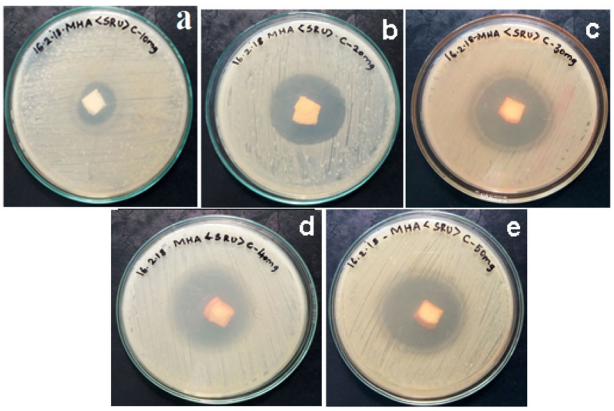

Keywords PVA · Starch · Hydrogel · Drug delivery · Biological activity · Cytotoxicity

✉ V. Parthasarathy
parthu0406@gmail.com

[1] Department of Food Technology, Hindustan Institute of Technology and Science, Padur 603103 Tamil Nadu, India

[2] Department of Physics, Hindustan Institute of Technology and Science, Padur 603103 Tamil Nadu, India

[3] Centre for Research & Consultancy, Department of Microbiology, Hindustan College of Arts & Science, Padur 603103 Tamil Nadu, India

Highlights

- The PVA/mannitol hydrogel was prepared to study its drug delivery potential.
- The PM hydrogel effectively delivered the drugs against MCF-7 and pathogenic strains.
- The PM hydrogel exhibited an excellent water retention ability.
- The prepared PM hydrogel was non-hemolytic to red blood cells.

1 Introduction

Hydrogels are the cross-linked structure of hydrophilic polymer chains that can hold a huge amount of water contents by retaining their chemical structure even in the swollen state. They are considered as promising materials in the manufacturing of hygiene products, contact lenses, wound dressings, drug delivery systems and tissue engineering scaffolds due to their flexibility similar to living tissues and biocompatibility [1]. The healing of a wound is associated with various complex biological processes such as inflammation, hemostasis, remodeling of damaged tissue, and proliferation [2]. The preparation of hydrogels is associated with the physical or chemical crosslinking of hydrophilic polymer chains. The natural or synthetic polymers having hydrophilic groups are used to develop bio-medically important hydrogels with high water content [3]. The requirements of hydrogels generally vary based on their applications. PVA is a synthetic hydrophilic polymer that plays a significant role in biomedical applications owing to its biocompatibility and biodegradability [4, 5]. PVA hydrogels have been employed in wound repair as they heal wound faster than the conventional cotton-based materials. However, the applications of PVA hydrogel are restricted by its incomplete hydrophilicity and poor stiffness. The physical and biological properties of PVA hydrogels can be enhanced by grafting or blending them with natural polymers. Starch is a natural polymer that is blended with PVA hydrogels to enhance the properties of PS hydrogel in this research work.

PVA hydrogel was proposed as a soft tissue substitute because its microstructure is similar to porcine liver tissue [6]. PVA hydrogels were investigated for their use in the development of artificial cornea [7]. The developed porous PVA/chitosan hydrogel was employed in the cartilage healing treatment [8]. The review on the applications of PVA-based hydrogel in wound dressing and tissue engineering was reported in the literature [9, 10]. Shitole et al. [11] investigated the physico-chemical properties of PVA-based hydrogels to evaluate their wound healing potential. PVA/alginate-based scaffold was reported as a promising bone wound healing material [12]. The colon-targeted drug release activity of starch-based hydrogel was studied by Liu and his research team [13]. Kunal et al. [14] reported that the PVA/starch membrane hydrogel enhanced the wound healing rate remarkably, and they also studied its biocompatibility on human breast cancer cell lines (MCF-7). The wound healing applications of the nanofibrous starch-based scaffold were reported by Vijaya and co-workers [15]. The antibacterial activity of PVA/starch hydrogel loaded with turmeric was evaluated against Gram-positive (*Staphylococcus aureus*) and Gram-negative (*E. coli*) bacterial strains [16]. The gentamicin drug-loaded PVA/dextran hydrogel was prepared to evaluate its in vivo wound healing potential [17]. The effect of chitosan on the physical–chemical properties of PVA/chitosan hydrogel was studied by Yang et al. [18]. The stable starch-based hydrogels were developed by Dominique et al. [19]. The applications of polysaccharide-based hydrogel in the biomedical field were reviewed in detail by Tianxue and his research group [20]. The studies about the investigation of the physical and biological properties of PVA-starch hydrogel are scarce in the open literature. This research also intends to analyze the drug release efficiency of PVA-starch hydrogel against the pus-inducing pathogenic strains and MCF-7 cells (breast cancer cell line). It is finally concluded that the prepared PVA-starch hydrogel can be used as promising dressing materials for wounds as well as radiotherapy burns to accelerate the healing process.

2 Experimental

2.1 Materials

Poly(vinyl) alcohol and starch were procured from Merck, India. The formaldehyde and conc. sulfuric acid were supplied by SD Fine chemicals, India. *Staphylococcus aureus* (MCC no: 2043) and MCF-7 cell line were received from National Center for Cell Science, Pune, India.

2.2 Preparation of PVA-starch hydrogel

The preparation of PVA-starch hydrogel was employed by the sol-gel techniques. The PVA aqueous solution was prepared by dissolving 1 g of PVA in 10 ml double distilled (DD) water. Then it was mixed with 10 ml of the prepared starch (250 mg) solution. This reaction mixture was further added with 2 ml of sulfuric acid and 1.4 ml of formaldehyde to initiate the formation of the hydrogel. Afterwards, it was poured onto a petri dish to obtain it as a thick sheet of the hydrogel. The casted PS hydrogel was dried at 50 °C for 2 h to carry out the analysis.

2.3 Characterization

The FTIR spectra of PVA and PS hydrogel had been captured by using the JASCO FTIR 4100 spectrometer in the wavenumber region of 400 to 4000 cm^{-1} to comprehend their chemical structure. The XRD patterns of PVA and its hydrogel had also been recorded on Brucker K 8600 instrument using CuKα radiation with the wavelength of $\lambda = 1.5405$ Å in the 2θ range from 20° to 100° to conclude their structure. The thermal decomposition behavior of PS hydrogel had been analyzed by investigating the recorded thermograms on TG/DTA 6200 thermal analyzer in the temperature range of 30 to 300 °C.

2.4 In-vitro degradation level

The PS hydrogel sample was cut into small pieces with the same dimension. All the pieces are incubated in a 2% lysozyme-containing phosphate buffer solution (PBS) to carry out this analysis for around 7 h. Afterwards, the incubated samples in the buffer solution were taken out and rinsed with double distilled water. The samples were dried to measure their final weight. The % degradation was determined using the mathematical relation as given below.

$$Degradation\ rate(S\%) = \frac{W_o - W_t}{W_o} \times 100 \quad (1)$$

where W_o - initial weight and W_t - swollen weight at time t

2.5 Swelling index

The PS hydrogels of dimension 4 cm^2 were allowed to soak in a PBS solution for a maximum of 1 h. Then the samples were collected with the help of blunt forceps at a constant time interval of 5 min to assess the swelling rate of hydrogel with respect to time. The weight of the collected samples was estimated after the removal of excess fluid from their surface. The swelling index was computed by using Eq. 2.

$$Swelling\ index\ (SI) = \frac{W_2 - W_1}{W_1} \times 100 \quad (2)$$

where W_1 and W_2 are the initial and final weight of the samples respectively. This experiment was performed thrice to obtain the mean value of the swelling index for the prepared hydrogel.

2.6 Moisture loss

The PS hydrogel stripes of dimension 4 cm^2 were taken to perform a moisture loss study. All the hydrogels strips were kept in a desiccator loaded with $CaCl_2$. The weight of the samples was recorded at a regular interval of 1 h until obtaining a constant weight. The difference between the initial and final weight of the strips was used to assess the rate of moisture loss by the hydrogels.

2.7 Hemolysis

Hemolysis is an important parameter as it describes the erythrocytic membrane (red blood cells) damages. The release of hemoglobin in the blood plasma concludes the red cell damages in the blood. An in-vitro hemolytic potential of PS hydrogel was evaluated by hemolytic analysis. The PS hydrogel was equilibrated in the saline solution at 37 ± 0.5 °C for 24 h. The acid-citrate-dextrose (ACD) blood (0.25 ml) was kept on the PS hydrogel to carry out this analysis. Then, 2 ml of saline solution was added to the hydrogel after 20 min. The sample was further incubated for 1 h at 37 ± 0.5 °C. The human ACD blood and saline solution were used as positive and negative controls respectively for this analysis. The optical density of the incubated samples was recorded at 545 nm. The % hemolysis was estimated using Eq. 3. The absorbance values are 1.25 for positive and 0.010 for negative controls.

$$Hemolysis\ (\%) = \frac{absorbance\ of\ test\ sample - absorbance\ of\ negative\ control}{absorbance\ of\ positive\ control - absorbance\ of\ negative\ control} \times 100 \quad (3)$$

2.8 Blood clot

The evaluation of the antithrombogenic property of PS hydrogel was done by blood clot analysis. The saline solution was used to equilibrate the PS hydrogel for 24 h at 37 °C. 0.5 ml of ACD-human blood was poured on the PS hydrogel. Then, 0.03 ml of calcium chloride solution was added to the blood sample to initiate the formation of a blood clot (thrombus). The thrombus formation was arrested by the addition of 4 ml of DD water. The clotted blood was separated by choking the hydrogel in DD water for 10 min at 30 °C. The collected thrombus was immersed in 2 ml of 36% formaldehyde solution. Then it was put in DD water for another 10 min. The weight of the thrombus was measured after drying it completely. The thrombus formation on the glass was also evaluated by the same method.

2.9 Antimicrobial drug delivery

The PS hydrogel was loaded with the different concentrations of cephalosporin drug (10–50 mg) to assess its antimicrobial drug release potential against pus-inducing pathogen, *Staphylococcus aureus* (MCC strain-no: 2043) by disc diffusion technique according to the CLSI guidelines. In brief, Mullar Hinton Agar media was prepared and the test organism was swabbed. The drug-loaded PS hydrogel

was impregnated and allowed for incubation at 37 °C for 24 h. The inhibitory zones were measured using the zone measuring scale.

2.10 In-vitro cytotoxicity

The cell viability, proliferation and cytotoxicity were examined by MTT assay. This analysis was intended to inspect the effect of curcumin-loaded PS-hydrogel against immortalized cell line of MCF-7 (breast cancer cells). The cultivation of MCF-7 was performed in a growth medium under humidified atmosphere. The cells were allowed to grow until the development of 80% confluent. Afterwards, the seeding of grown cells was carried out in a 96 well plate under humidified atmosphere for incubation.

2.11 MTT assay

MTT reduction assay was performed to conclude the viability of the cells. The sample solutions were drained off from the well and 50 µl of diluted MTT in PBS was added to the well. Then, it was incubated at 37 °C in a 5% CO_2 atmosphere. After removal of the supernatant, 100 µl of DMSO was added to check the formation of formazan. The plate was read at 540 nm using micro-plate reader.

3 Results and discussion

3.1 FTIR study

Figure 1a depicts the FTIR spectrum of PVA. A peak at 3366 cm^{-1} is associated with the O–H (hydroxyl) group of PVA. The asymmetric mode of C–H stretching is noticed at 2930 cm^{-1}. The C=O (carbonyl) stretching of PVA occurs at 1731 cm^{-1} [21]. The $–CH_2$ bending and wagging modes of vibrations assign in the wavelength regions of 1414 and 1386 cm^{-1} respectively. The C–H wagging vibration is seen at 1575 cm^{-1}. The peaks at 1080 and 835 cm^{-1} are attributed to the stretching modes of C–O–C and $–CH_2$ vibrations. The FTIR spectrum of starch is demonstrated in Fig. 1b. The C–O stretching of C–O–C groups in starch is noticed at 1020 cm^{-1} [22]. A peak at 1090 cm^{-1} is associated with the C–O stretching of C–OH groups. The skeletal modes of the pyranose ring of glucose unit occur in the wavelength regions of 629 and 548 cm^{-1}. A peak at 3239 cm^{-1} is attributed to the O–H group's stretching vibration [23]. The bending mode of C–H vibration is noticed at 1432 cm^{-1} for starch. Figure 1c depicts the FTIR spectrum of PS hydrogel. The strong interaction between the PVA and starch occurs through their hydroxyl groups. The peak corresponding to the hydroxyl group of PVA at 3366 cm^{-1} becomes broader after blending with PVA. This is due to the formation of intermolecular bonds between the PVA and starch.

3.2 XRD study

The structure of the PVA and PS hydrogels was also inspected by analyzing their XRD patterns. The XRD pattern of PVA is portrayed in Fig. 2a. A broad peak at 19.8° is mainly due to the reflection of the (110) crystal plane of PVA. It proves the semicrystalline nature of PVA [24]. Starch is a polysaccharide that exhibits semicrystalline nature. It is understood from the assigned diffraction peaks of starch at 20° and 45° as illustrated in Fig. 2b. The XRD profile of PS hydrogel is depicted in Fig. 2c. The characteristics peaks of PVA and starch are not seen in the XRD

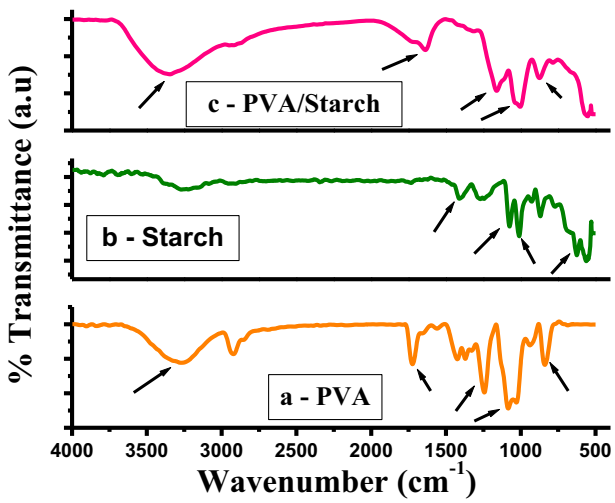

Fig. 1 FTIR spectra of (**a**) pristine PVA, (**b**) starch, and (**c**) PS hydrogel

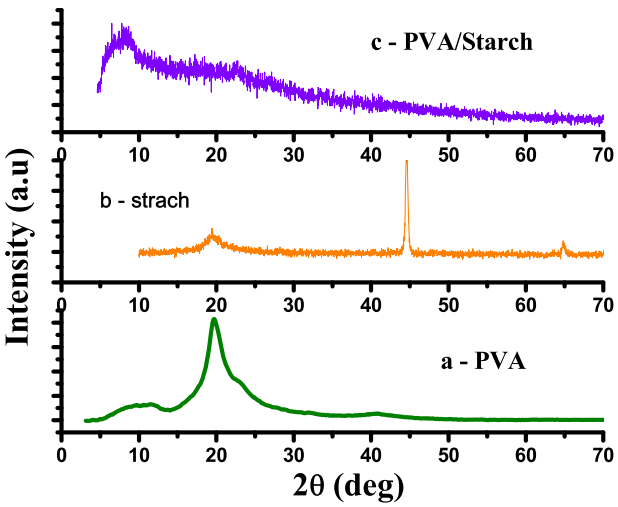

Fig. 2 XRD profiles of (**a**) pristine PVA, (**b**) starch, and (**c**) PS hydrogel

pattern of PS hydrogel as the semicrystalline nature of PVA is transformed into amorphous due to the interaction of starch with the PVA matrix.

3.3 TGA analysis

The thermal stability of PS hydrogel was investigated by comparing its TG thermograms with pristine PVA. The TG thermogram of PVA exhibits two-step decomposition processes as shown in Fig. 3a. The maximum decomposition temperature (T_d) is observed at 171 °C for the first step. There is a minor mass loss due to the elimination of the physically and chemically bounded water molecules. The second-step decomposition is accompanied by the major mass loss owing to the decomposition of the PVA backbone. Figure 3b demonstrates the TG thermogram of PS hydrogel. The decomposition of PS hydrogel occurs in two steps with the elimination of water molecules in the first step and the degradation of the PVA backbone in the second step. The degradation temperature of PS hydrogel is almost equal to the T_d of pristine PVA for the first step. It is noted that the second-step decomposition process starts at 276 °C and extends up to 480 °C for PS hydrogel, while it is in the range of 287 to 484 °C for PVA. The % weight residue remains above 500 °C is 8% for PS hydrogel which is found to be higher as compared with the % weight residue of PVA (3.7%). There is a slight decrement in the thermal stability of PS hydrogel in the second step as compared with PVA. However, the obtained % weight residue is higher for PS hydrogel while comparing it with PVA

3.4 In-vitro degradation level

During the wound repairing activity, the healing materials should not produce any secondary chemicals that delays angiogenesis. Figure 4 illustrates the variation in the in-vitro biodegradation (S%) of PS hydrogel with time. The standard deviation (SD) was estimated as 2%. There is a minimal weight reduction in the PS hydrogel sample while incubating it in 0.2% of lysozyme-containing PBS solution for 7 h at pH 7 (Fig. 4). The slower weight loss of PS hydrogel in PBS solution concluded that it is biodegradable but stable in physiological conditions. This increased enzymatic stability is one of the significant important parameters for dressing materials [25]. Therefore, the PS hydrogel is an ideal material for wound dressing due to its proven enzymatic stability.

3.5 Swelling index

The swelling index of PS hydrogel was found to be increased by 160% within 40 min and then to 230% in 70 min as compared its dried weight (Fig. 5). It proved that the water absorption rate of PS hydrogel took place slowly. The SD was determined as 4.7%. The equilibrium swelling of PS hydrogel was obtained after 7th h of incubation in pure water. Therefore, the prepared PS hydrogel is a potential candidate for wound dressing applications due to its excellent water absorption potential. Moreover, the PS hydrogel can accelerate the wound healing process by offering a moist environment around the wound site which generally prevents the damaged skin from angiogenesis and cellular hydration [26].

3.6 Moisture loss study

The PS hydrogel was also investigated to assess its dehydration potential under desiccation conditions by measuring the weight of the hydrogel at regular intervals of time. The prepared PS hydrogel exhibited a poor water loss over a

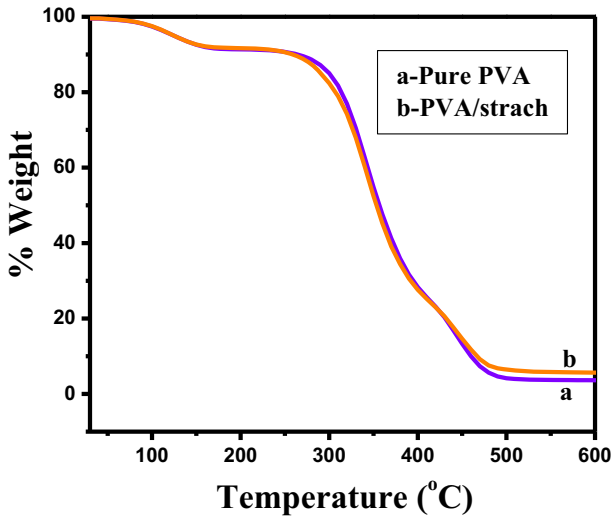

Fig. 3 TG thermograms (**a**) pristine PVA, (**b**) PS hydrogel

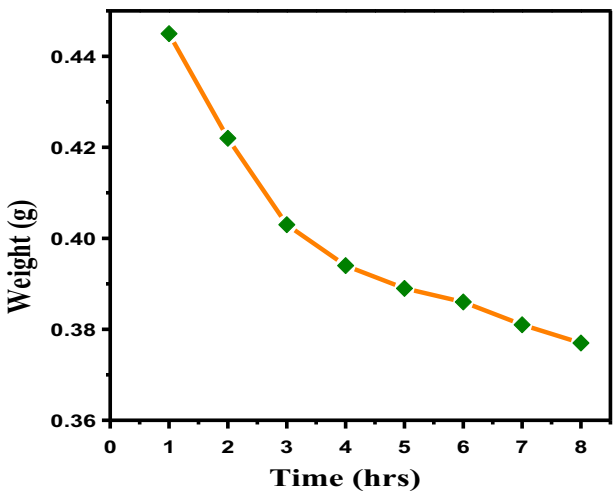

Fig. 4 Biodegradation potential of the PVA-starch hydrogel membrane

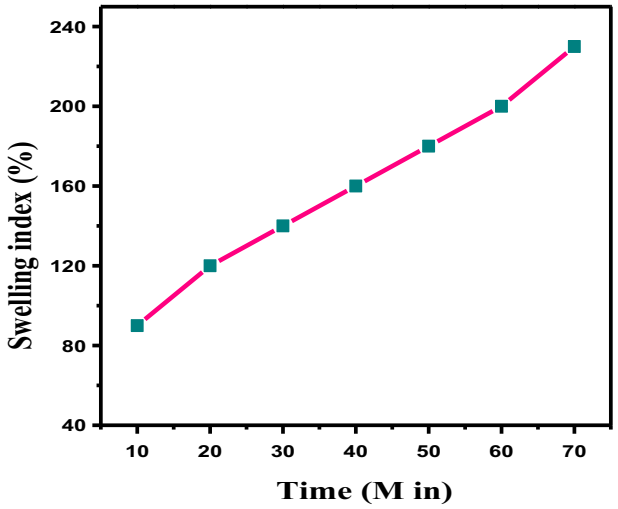

Fig. 5 Water absorbing capacity of the PVA-starch hydrogel membrane

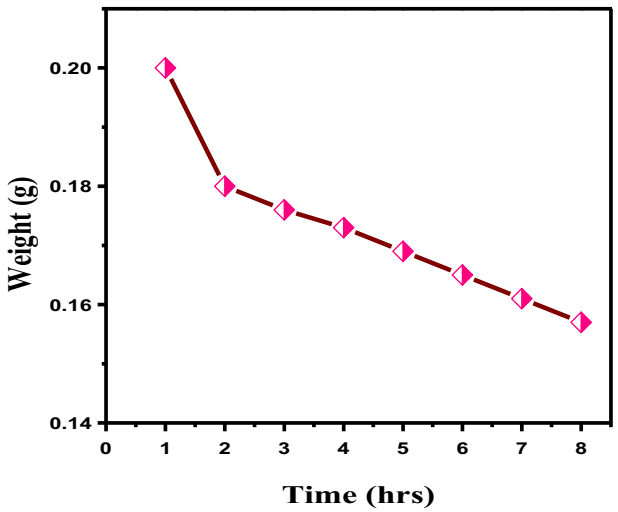

Fig. 6 Moisture loss analysis of PVA-Starch hydrogel

period of time as shown in Fig. 6. This proves that the water retention ability of PS hydrogel is considerably high. Meantime, the dehydration of PS hydrogel occurred while placing it for a long time in a desiccator. This property of the hydrogel helps to absorb water content from the wound exudates [27]. The obtained SD value was 1.3%.

3.7 Hemocompatibility and blood clot analysis

The percentage of hemolysis was <3.09% for the prepared PS hydrogel. Hence, there was no erythrocytic membrane damage by the PS hydrogel. It was found to be non-hemolytic for red blood cells (RBC). Therefore, PS hydrogel can be used as wound dressing materials (Fig. 7a, b).

The antithrombogenicity is one of the important characteristics of blood-contacting materials. The antithrombogenicity

Fig. 7 **a** Hemolysis analysis. **b** Blood clot analysis of PS hydrogel

of PS hydrogel was evaluated by analyzing the thrombus formation on the wet polymeric hydrogel. The thrombus formation (blood clot) increased the weight of the PS hydrogel by 0.5% while placing ACD blood on the hydrogel specimen. The formation of a thrombus on the glass surface increased its weight by 3.5%. The fibrin clot deposition was lower for PS hydrogel as compared with glass. There was no high level of thrombus formation by the PS hydrogel. Hence, the PS hydrogel is a potential candidate for wound healing applications [27].

3.8 Drug delivery efficacy of PS hydrogel bacterial strains

The cephalosporin-loaded PS hydrogel was investigated to assess its antimicrobial potential against *Staphylococcus aureus* (MCC No: 2043) by disc diffusion method. The zone of inhibition was measured after 24 h. The drug-loaded PS hydrogel effectively delivered the cephalosporin against *S. aureus*. The zone of inhibition was found to be increased with the increasing concentration of the drug as shown in Fig. 8a–e. The release of cephalosporin from the PS hydrogel took place at a controlled rate due to the intermolecular interaction between the PS hydrogel and antibiotic [28, 29]. The drug delivery potential of PS hydrogel against pathogenic microorganisms was concluded by this analysis.

3.9 Drug delivery efficacy against cancer cells

The curcumin was loaded onto the PS hydrogel to analyze its cytotoxicity against cancer cells. The curcumin-loaded PS hydrogel exhibited a significant anticancer activity as 92.7% of cancer cells became nonviable after 7 days while exposing to the drug-loaded PS hydrogel. In 3rd, 5th and 7th days of incubation, MCF-7 alive cells were highly restricted by curcumin treated sample as compared with a control sample (Table 1). Meantime, the percentage of nonviable cells was increased with the incubation time for curcumin treated sample as compared with a control sample (Table 1). The cancerous cell growth was considerably

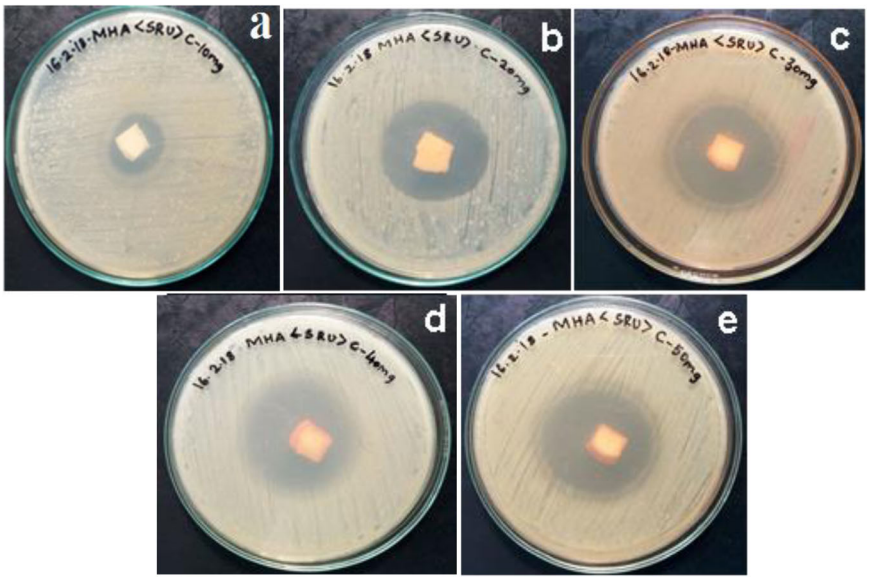

Fig. 8 Cephalosporin drug delivery potential of PS hydrogel against pathogenic *Staphylococcus aureus (MCC No: 2043)*

Table 1 PVA-starch hydrogel cytotoxicity analysis on MCF-7 cells

Days	Sample	Alive cells (%)	Nonviable cells (%)
3rd Day	Control	96.3	9.1
	Treated	3.5	79.6
5th Day	Control	89.7	13.1
	Treated	8.1	87.5
7th Day	Control	88.9	19.2
	Treated	12.2	92.7

inhibited by the 1% curcumin-loaded PS hydrogel. The controlled release of curcumin from the PS hydrogel greatly reduced the cell growth by 79.6% on the 3rd day of incubation. The percentage of alive cancerous cells was only 12.2% on the 7th day of incubation. However, the cell growth started increasing after the 7th day of incubation. The increase in cell growth concluded that the curcumin was effectively released only up to the 5th day by the PS hydrogel membrane. Therefore, the curcumin-loaded PS hydrogel can be used in treating the wounds of cancer patients [30, 31].

4 Conclusion

The drug release potential of PS hydrogel was examined against MCF-7 cells and pathogenic strain (*S. aureus*). The FTIR analysis concluded that the broadening of the peak corresponding to the hydroxyl groups of PVA was due to the interaction of starch and PVA through their hydroxyl groups. The T_d of PVA and PS hydrogel was at 171 °C for the first-step decomposition process. The decrement in the thermal stability of PS hydrogel in the second step and the increment in the obtained % weigh residue above 500 °C were concluded from the TGA analysis by comparing that with PVA. The PS hydrogel exhibited an excellent water absorption potential and so that can prevent cellular dehydration while using it as dressing materials. The PS hydrogel had not induced any cell damage to RBC as the % of hemolysis was <3.09%. The prepared PS hydrogel showed a remarkable antithrombogenic potential as the fibrin clot deposition increased the weight of PS hydrogel by only 0.5%. The pus-inducing pathogen of *S. aureus* (MCC strain-no: 2043) was effectively inhibited by the PS hydrogel when loaded with cephalosporin. The PS hydrogel loaded with curcumin delivered the drugs at the controlled rate against MFC-7 cells and also inhibited the growth of cancerous cells by killing around 92.7% of cells even after the 7th day of inhibition. The drug-loaded PS hydrogel can be used as a wound dressing material for both noncancerous and cancer-treated radiotherapy wounds.

Compliance with ethical standards

Conflict of interest The authors declare no competing interests.

Publisher's note Springer Nature remains neutral with regard to jurisdictional claims in published maps and institutional affiliations.

References

1. Caló E, Khutoryanskiy VV (2015) Biomedical applications of hydrogels: a review of patents and commercial products. Eur Polym J 65:252–267. https://doi.org/10.1016/j.eurpolymj.2014.11.024
2. Kurhade S, Momin M, Khanekar P, Mhatre (2013) Novel biocompatible honey hydrogel wound healing sponge for chronic ulcers. Int J Drug Deliv 5:353–361

3. Silva AKA, Richard C, Bessodes M, Scherman D, Merten OW (2009) Growth factor delivery approaches in hydrogels. Biomacromolecules Biomacromol 10(1):9–18. https://doi.org/10.1021/Bm801103c
4. Chen DH, Leu JC, Huang TC (1994) Transport and hydrolysis of urea in a reactor–separator combining an anion exchange membrane and immobilized urease. J Chem Technol Biotechnol 61:351–357
5. Hyon SH, ChaWI, Ikada Y, KitaM, Ogura Y, Honda Y (1994) Poly (vinyl alcohol) hydrogels as soft contact lens material. J Biomater Sci Polym Ed 5:397–406. https://doi.org/10.1163/156856294x00103
6. Shan J, Liu S, Wenhao F (2011) PVA hydrogels properties for biomedical application. J Mech Behav Biomed Mater J Mech Behav Biomed Mat 4(7):1228–1233. https://doi.org/10.1016/j.jmbbm.2011.04.005
7. Yi H, Chen C, Kemin L, Ying T, Zhang L, Yubao L (2015) Preparation of PVA hydrogel with high transparency and investigations of its transparent mechanism. RSC Adv 31 (5):24023–24030. https://doi.org/10.1039/C5RA01280E
8. Peng L, Zhou Y, Lu W et al. (2019) Characterization of a novel polyvinyl alcohol/chitosan porous hydrogel combined with bone marrow mesenchymal stem cells and its application in articular cartilage repair. BMC Musculoskelet Disord 20:257. https://doi.org/10.1186/s12891-019-2644-7
9. Anuj K, Sung SH (2016) PVA-based hydrogels for tissue engineering: a review. Int J Polym Mater Polym Biomater Int J Polym Mat Polym Biomat 66(4):159–182. https://doi.org/10.1080/00914037.2016.1190930
10. Elbadawy AK, El-Refaie SK, Xin C (2017) A review on polymeric hydrogel membranes for wound dressing applications: PVA-based hydrogel dressing. J Adv Res 8(3):217–233. https://doi.org/10.1016/j.jare.2017.01.005
11. Shitole AA, Raut PW, Khandwekar A et al. (2019) Design and engineering of polyvinyl alcohol based biomimetic hydrogels for wound healing and repair. J Polym Res 26:201. https://doi.org/10.1007/s10965-019-1874-6
12. Bahadoran M, Shamloo A, Nokoorani YD (2020) Development of a polyvinyl alcohol/sodium alginate hydrogel-based scaffold incorporating bFGF-encapsulated microspheres for accelerated wound healing. Sci Rep. 10:7342. https://doi.org/10.1038/s41598-020-64480-9
13. Liu C, Gan X, Chen Y (2010) A novel pH-sensitive hydrogels for potential colon-specific drug delivery: Characterization and in-vitro release studies. Starch Stark 63(8):503–511. https://doi.org/10.1002/star.201000120
14. Kunal P, Ajith B, Dipak KM (2006) Preparation of transparent starch based hydrogel membrane wit potential application as wound dressing. Trend Biomat Artif Organ 20(1):59–57
15. Vijaya SW, Pallavi RW, Sathish D, Aparna D, Ratnesh J, Prajakta D (2018) Starch based nanofibrous scaffolds for wound dressing applications Bioact Mater Bioact Mater 3(3):255–266. https://doi.org/10.1016/j.bioactmat.2017.11.006
16. Awais H, Niazi MBK, Arshad H, Sarah F, Tahir A (2018) Development of anti-bacterial PVA/starch based hydrogel membrane for wound dressing. J Polym Environ 26:235–243. https://doi.org/10.1007/s10924-017-0944-2
17. Hwang M-R, Kim JO, Lee JH et al. (2010) Gentamicin-loaded wound dressing with polyvinyl alcohol/dextran hydrogel: gel characterization and in vivo healing evaluation. AAPS PharmSciTech 11:1092–1103. https://doi.org/10.1208/s12249-010-9474-0
18. Yang JM, Su WY, Leu TL, Yang MC (2004) Evaluation of chitosan/ PVA blended hydrogel membranes. J Membr Sci 236:39–51. https://doi.org/10.1016/j.memsci.2004.02.005
19. Dominique LW, Isabel S, Giovanna F (2020) Starch-based hydrogels produced by high-pressure processing (HPP): effect of the Starch Source and Processing Time. Food Eng Review https://doi.org/10.1007/s12393-020-09264-7
20. Tianxue Z, Jiajun M, Yan C, Haoran L, Lu L, Mingzheng G, Shuhui L, Jianying H, Zhong C, Huaqiong L, Lei Y, Yuekun L (2019) Recent progress of polysaccharide-based hydrogel interfaces for wound healing and tissue engineering. Advan Mat Inter 6 (17):e1900761. https://doi.org/10.1002/admi.201900761
21. Selvi J, Parthasarathy V, Mahalakshmi S, Anbarasan R, Kumar PS, Daramola MO (2019) Enhancement in thermal, mechanical and electrical properties of novel PVA nanocomposite embedded with SrO nanofillers and the analysis of its thermal degradation behavior by nonisothermal approach. Poly Compos 1–14. https://doi.org/10.1002/pc.25453
22. Huafeng T, Jiaan Y, Varada R, Aimin X, Xiaogang L (2017) Fabrication and properties of polyvinyl alcohol/starch blend films: effect of composition and humidity. Int J Biol Macromol 96:518–523. https://doi.org/10.1016/j.ijbiomac.2016.12.067
23. Jeiffer FV, José GE, Vidala MV, Jorgelina P, Pedro MC, Henry ALM (2018) Chemical Modification and Characterization of Starch Derived from Plantain (*Musa paradisiaca*) Peel Waste, as a Source of Biodegradable Material, Chemical Engineering Transactions. Chem Eng Transact 65 https://doi.org/10.3303/CET1865128
24. Selvi J, Parthasarathy V, Mahalakshmi S, Anbarasan R, Daramola MO, Senthil KP (2020) Optical, electrical, mechanical, and thermal properties and non-isothermal decomposition behavior of poly(vinyl alcohol)—ZnO nanocomposites. Iran Polym J 29:411–422. https://doi.org/10.1007/s13726-020-00806-8
25. Ng KW, Achuth HN, Moochhala S, Lim TC, Hutmacher DW (2007) In vivo evaluation of an ultra-thin polycaprolactone film as a wound dressing J Biomat Sci Polym Ed 18(7):925–938. https://doi.org/10.1163/156856207781367693
26. Bárbara B, Wyller MF, Rosana C, Shanise L, Loong-Tak L, Álvaro RG, Elessandra Z (2018) Starch hydrogels: the influence of the amylose content and gelatinization method. Intern J Biol Macromol 113:443–449. https://doi.org/10.1016/j.ijbiomac.2018.02.144
27. Todor TK, Juan CMG, DinuIuga YZ, Khimyak FJW (2020) Structural heterogeneities in starch hydrogels. Carb Polym 249:116834. https://doi.org/10.1016/j.carbpol.2020.116834
28. Tavakoli J, Mirzaei S, Tang Y (2018) Cost-effective double-layer hydrogel composites for wound dressing applications. Polymer 10 (3):305. https://doi.org/10.3390/polym10030305
29. Kerong Y, Qing H, Bingpeng C, Yuhao Z, Kesong Z, Qiang L, Jincheng W (2017) Antimicrobial hydrogels: promising materials for medical application. Int J Nanomed 13:2217–2263. https://doi.org/10.2147/IJN.S154748
30. Parviz DM, Shiva AB, Saeed M, Foad K, Nasser N, Mohsen N, Seyed AM (2020) Synthesis, characterization, and in-vitro evaluation of the starch-based α-amylase responsive hydrogels. J Cell Phy 236(5):4066–4075. https://doi.org/10.1002/jcp.30148
31. Jun-Li L, Yan-Y P, Ou C, Yun L, Xia X, Jing-Jie Z, Ling L, Hong-Ying J (2017) Curcumin inhibits MCF-7 cells by modulating the NF-κB signaling pathway Oncol Lett 14 (5):5581–5584. https://doi.org/10.3892/ol.2017.6860